REPORT

MCM9 Mutations Are Associated with Ovarian Failure, Short Stature, and Chromosomal Instability

Michelle A. Wood-Trageser,[1] Fatih Gurbuz,[2] Svetlana A. Yatsenko,[1,3] Elizabeth P. Jeffries,[4] L. Damla Kotan,[5] Urvashi Surti,[1,3] Deborah M. Ketterer,[1] Jelena Matic,[1] Jacqueline Chipkin,[1] Huaiyang Jiang,[1] Michael A. Trakselis,[4,7] A. Kemal Topaloglu,[2] and Aleksandar Rajkovic[1,3,6,*]

Premature ovarian failure (POF) is genetically heterogeneous and manifests as hypergonadotropic hypogonadism either as part of a syndrome or in isolation. We studied two unrelated consanguineous families with daughters exhibiting primary amenorrhea, short stature, and a 46,XX karyotype. A combination of SNP arrays, comparative genomic hybridization arrays, and whole-exome sequencing analyses identified homozygous pathogenic variants in *MCM9*, a gene implicated in homologous recombination and repair of double-stranded DNA breaks. In one family, the *MCM9* c.1732+2T>C variant alters a splice donor site, resulting in abnormal alternative splicing and truncated forms of MCM9 that are unable to be recruited to sites of DNA damage. In the second family, *MCM9* c.394C>T (p.Arg132*) results in a predicted loss of functional MCM9. Repair of chromosome breaks was impaired in lymphocytes from affected, but not unaffected, females in both families, consistent with *MCM9* function in homologous recombination. Autosomal-recessive variants in *MCM9* cause a genomic-instability syndrome associated with hypergonadotropic hypogonadism and short stature. Preferential sensitivity of germline meiosis to MCM9 functional deficiency and compromised DNA repair in the somatic component most likely account for the ovarian failure and short stature.

In premature ovarian failure (POF [MIM 311360]), ovaries cease to produce mature oocytes prior to 40 years of age.[1,2] The condition is characterized by secondary amenorrhea, infertility, hypoestrogenism, and elevated serum levels of follicle-stimulating hormone (FSH). POF is heritable in up to 30% of individuals.[3] Pathogenesis of POF includes abnormalities of the X chromosome or autosomes and can also be due to autoimmune, infectious, and environmental causes.[1,2] For a subset of idiopathic cases, a genetic basis has been shown, and *FMR1* (MIM 309550), *FSHR* (MIM 136435), *PMM2* (MIM 601785), *GALT* (MIM 606999), *AIRE* (MIM 607358), and *FOXL2* (MIM 605597) are the only genes currently recommended for clinical genetic testing.[2,4] In cases of short stature and POF, karyotype is usually performed for ruling out 45,X or Turner syndrome, and subsequent evaluation depends on the clinical presentation. Several genomic-instability disorders are known to associate with short stature and hypogonadism and include Bloom syndrome (MIM 210900),[5] Fanconi anemia (MIM 227650),[6] ataxia telangiectasia (MIM 208900),[7] and Nijmegen breakage syndrome (MIM 251260).[8]

We separately investigated two independent consanguineous Turkish families of Kurdish ethnicity for primary amenorrhea (the absence of menstruation) in their daughters (Figures 1A and 1B). Peripheral-blood samples were obtained from affected (AII-4, AII-6, and BII-1) and unaffected (AI-1, AI-2, AII-1, AII-2, AII-3, AII-5, AII-7, BI-1, BI-2, BII-2, BII-3, and BII-4) family members. The study was approved by the ethics committee of the Cukurova University Faculty of Medicine, and informed written consent was obtained from all participating subjects.

In family A, the parents are first-degree cousins. The mother (AI-2) entered menarche at 15 years of age, reported normal pubertal development, and continues to have regular menstrual periods (26- to 28-day menstrual cycles) at 49 years of age. She had no difficulties becoming pregnant and is currently 150 cm tall and weighs 68 kg. She gave birth to six girls and one boy. Two of her daughters (AII-4 and AII-6) were initially clinically evaluated for a Turner-like phenotype of primary amenorrhea and short stature (Figure 1A). All clinical investigations are described in Table S1 (available online). In summary, the affected daughters presented with hypergonadotropic primary amenorrhea, short stature, low weight, and a normal 46,XX karyotype. Estradiol levels were low, whereas luteinizing hormone (LH) and FSH levels were high. Prolactin levels were normal. Ovaries were not identified on pelvic ultrasound, and the uteri were infantile. Both individuals are currently regularly menstruating on combined estrogen-progestin replacement therapy and are achieving appropriate bone ages, pubic-hair stages, and Tanner stages of breast development. There is no known family history of anemia, blood dyscrasias, photosensitivity, immunodeficiency, or malignancies. Three unaffected sisters (AII-2, AII-3, and AII-5), aged 22–26 years, all entered menarche between the ages of 12 and 13 years and are currently experiencing regular menstrual cycles. The youngest sister,

[1]Department of Obstetrics, Gynecology, and Reproductive Sciences, Magee-Womens Research Institute, University of Pittsburgh, Pittsburgh, PA 15213, USA; [2]Division of Pediatric Endocrinology, Faculty of Medicine, Cukurova University, Adana 01330, Turkey; [3]Department of Pathology, University of Pittsburgh, Pittsburgh, PA 15261, USA; [4]Department of Chemistry, University of Pittsburgh, Pittsburgh, PA 15260, USA; [5]Department of Biotechnology, Institute of Sciences, Cukurova University, Adana 01330, Turkey; [6]Department of Human Genetics, University of Pittsburgh, PA 15261, USA
[7]Present address: Department of Chemistry and Biochemistry, Baylor University, Waco, TX 76798, USA
*Correspondence: rajkovic@upmc.edu
http://dx.doi.org/10.1016/j.ajhg.2014.11.002.

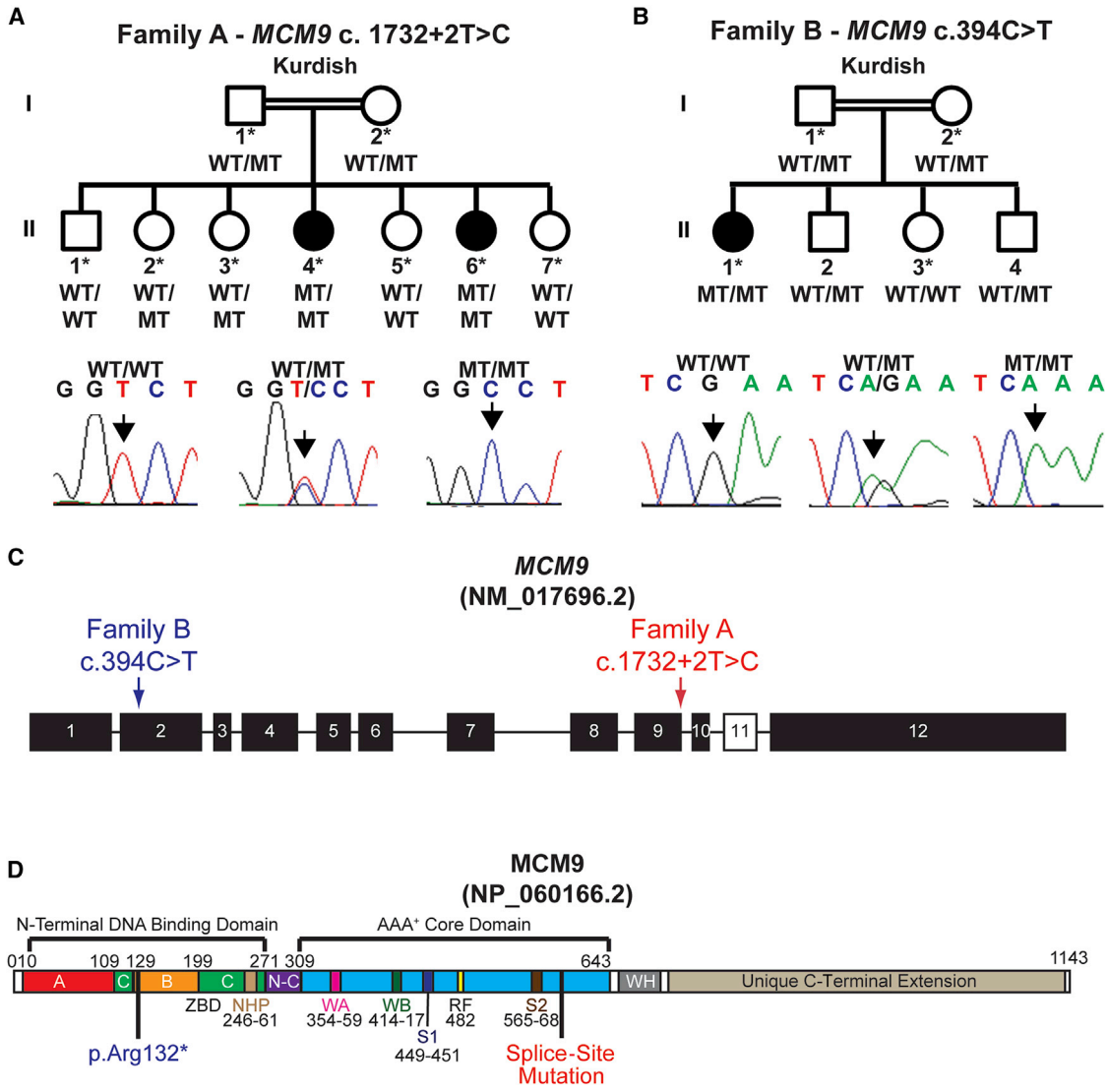

Figure 1. Pathogenic Homozygous Recessive Variants in *MCM9* Were Identified in Two Consanguineous Kurdish Families from Turkey

(A and B) The *MCM9* genotype is provided below each individual. WT denotes the wild-type allele. MT (for mutation) indicates either (A) *MCM9* c.1732+2T>C or (B) *MCM9* c. 394C>T. PCR amplification was completed with the KAPA HiFi HotStart PCR Kit with dNTPs (Kapa Biosystems) according to the manufacturer's instructions (primers for A are 5′-TCTAGGAGGTCCCGAGATGG-3′ and 5′-CAAAGGCA GAGTGATTGCCG-3′; primers for B are 5′-GCCTGAGAGGCAAGTGAATTTAG-3′ and 5′-TACCTAAAACCAAGGATGTGGGA-3′). PCR products were sequenced at Beckman Coulter Genomics. Results were analyzed with Sequencher (Gene Codes Corporation). Sample chromatograms are shown (5′ to 3′ direction in A; 3′ to 5′ direction in B). Arrows point to the nucleotide peak of interest. Samples utilized for whole-exome sequencing (WES) are indicated by an asterisk.

(C) *MCM9* is encoded on chr6: 119,252,903–119,134,612 (UCSC Genome Browser hg19). The *MCM9* c.1732+2T>C splice variant lies in the splice donor site of exon 9 (red arrow). The c.394C>T mutation lies near the 5′ end of exon 2 (blue arrow). Exons are indicated as full boxes (black). Alternative splice forms of *MCM9* either include or exclude exon 11 (white). Introns are indicated as lines.

(D) MCM9 consists of an N-terminal DNA binding domain and AAA^+ core domain. The c.1732+2T>C mutation is predicted to disrupt normal splicing after amino acid 577. The c.394C>T mutation causes insertion of a stop codon in the place of an arginine at position 132 (p.Arg132*). This most likely results in a truncated protein if one is formed. The yellow box represents the arginine finger domain (RF), the pink box represents the Walker A motif (WA), and the deep green box represents the Walker B motif (WB).

AII-7, presented with developmental delay and short stature, but not ovarian failure. She was excluded from further genetic analyses because of abnormal de novo chromosomal microarray findings (Figure S1), which most likely explain her phenotype.

An unrelated family B has a 16-year-old girl (BII-1; Figure 1B) with primary amenorrhea, short stature, and a lack of breast development. Her medical history is otherwise unremarkable. Clinical investigations are summarized in Table S1. She was found to have minimal breast development, stage III (P3) pubic hair, and stage II axillary-hair development. She had short stature, low weight, and a bone age of 11 years (Table S1). Pelvic ultrasonography revealed an infantile uterus and no visible ovaries. Her basal

estradiol level was low, whereas LH and FSH levels were elevated. Prolactin levels measured in the normal range. She has a normal 46,XX female karyotype. She has regular menstrual bleeding with combined estrogen-progestin replacement therapy. Hormone replacement therapy led to increased height, weight, and breast development. The proband's mother (BI-2) is currently 39 years of age. She exhibited signs of thelarche at 10 years of age and had normal first menarche at 13 years of age. She continues to cycle normally. She is 157.5 cm tall and weighs 61 kg. The 13-year-old unaffected sister (BII-3) had a normal first menarche at 12 years of age and has had regular menstrual cycles. Her height is 150.1 cm (−1.0 SD), and her weight is 37.4 kg (−1.1 SD). Additionally, the proband has two healthy brothers (BII-2 and BII-4) who have no known medical problems.

To identify the genetic cause of primary amenorrhea in family A, we performed DNA copy-number analysis and homozygosity mapping in two affected individuals (AII-4 and AII-6) and four unaffected female siblings (AII-2, AII-3, AII-5, and AII-7) by using a 180K comparative genomic hybridization (CGH) and SNP oligonucleotide array (SurePrint G3 ISCA design CGH+SNP, Agilent). The CGH+SNP microarray identified two contiguous regions of homozygosity on chromosomes 1 and 6: 1p34.3 (chr1: 35,187,876–36,929,988; UCSC Genome Browser hg19) and 6q21–q22.33 (chr6: 114,543,815–127,262,938; UCSC Genome Browser hg19). They were shared by the two affected daughters, but not by unaffected individuals (Figure S2). These two regions of homozygosity did not contain genes known to be associated with human ovarian failure and short stature. We therefore undertook an unbiased whole-exome sequencing (WES) approach to identify pathogenic variants.

We conducted WES on three unaffected daughters (AII-2, AII-3, and AII-5), both parents (AII-1 and AII-2), and two affected siblings (AII-4 and AII-6). Exons and splice sites were captured with the Agilent SureSelectXT Human Exon V4+UTRs Kit, and 2 × 100 bp paired-end WES was performed on an Illumina HiSeq 2500. Quality metrics for sequencing are shown in Table S2. We prepared reads for analysis with Cutadapt version 1.2.1 to remove the adapters and with the FASTX-Toolkit version 0.0.13.2 to trim the first 5 bp at the 5′ end of reads. We aligned data to UCSC Genome Browser hg19 by using Burrows-Wheeler Aligner version 0.7.3a MEM (maximal exact match).[9,10] Alignment statistics are presented in Tables S2 and S3. Local realignment around insertions and deletions, recalibration of read base quality, and variant calling were conducted with Genome Analysis Toolkit (GATK) version 2.6-5. GATK HaplotypeCaller was used for calling variants. Variant filtering is described in Table S4. The number of family members and availability of unaffected siblings enhanced the ability to filter gene variants that did not match an autosomal-recessive inheritance model. Three variants in *CEP85L* (6q22.31, RefSeq accession number NM_001042475), *GEMIN4* (17p13.3, RefSeq NM_015721), and *MCM9* (6q22.31, RefSeq NM_017696.2) fit the homozygous autosomal-recessive model (Table S5). *CEP85L* and *MCM9* mapped to the homozygosity region shared by affected sisters on chromosome 6 (Figure S2). The *CEP85L* variant (c. 497A>T [p.Asp166Val]) was previously reported as a SNP (rs9489444) with an allele frequency of 3% and is not conserved across species. We eliminated *CEP85L* as a likely cause of the observed phenotype.

The *MCM9* c.1732+2T>C variant (chr6: 119,149,088, UCSC Genome Browser hg19) changes an intron 9 splice donor site that is conserved at the nucleotide level across species including mouse, *Xenopus*, and zebrafish (Figures 1C and 1D). This variant is not present in either the NHLBI Exome Sequencing Project Exome Variant Server or 1000 Genomes. The *MCM9* c.1732+2T>C variant was confirmed by Sanger Sequencing (Figure 1A). A control population of women who were of European descent and who had at least one live birth was recruited at Magee-Womens Hospital. Written informed consent and samples were obtained and subsequently deidentified at the time of recruitment. The study was approved by the institutional review board of the University of Pittsburgh. The *MCM9* c.1732+2T>C mutation was not present in the 200 fertile women from this cohort.

We examined the effect of the c.1732+2T>C mutation on *MCM9* RNA alternative splicing products. mRNAs from Epstein-Barr-virus-transformed lymphoblastoid cell lines were generated from an unrelated control individual (wild-type), the unaffected mother (AI-2, heterozygous), and one affected daughter (AII-6, homozygous). RNA was isolated with Trizol (Invitrogen) and was reverse transcribed to cDNA with the SuperScript III First-Strand Synthesis Kit (Invitrogen). Using the KAPA HiFi HotStart PCR Kit with dNTPs (Kapa Biosystems) and primers to amplify exons 7–12 (c.1151_1996), we expected to observe two previously reported wild-type products: an 846 bp product and a 700 bp product resulting from exon 11 skipping[11] (Figure 2A; Figures S3B, S3C, and S4A). Indeed, we observed these two bands in the control individual (Figure 2B, left), and Sanger sequencing confirmed the expected exon order (Figures 2A and 2B; Figure S3B). In the heterozygous individual, we observed the 846 bp product, a faint 700 bp product, and three additional products, including two faint bands at 954 bp and 499 bp and a stronger band at 646 bp (Figures 2A and 2B). We were not able to detect either wild-type product in AII-6, the affected individual homozygous for the *MCM9* variant. Instead, we observed in this individual the three alternative bands (Figure 2B), which sequencing revealed to be abnormal splicing products. Using sequencing, we determined that the 954 bp band was composed of exons 8 and 9 plus 108 bp of downstream intronic sequence spliced onto exon 10 (Figure S3A). This intronic region ends at a cryptic splice site and is predicted to encode an additional 29 amino acids followed by a premature stop codon (Figure S4B), suggesting that truncated MCM9

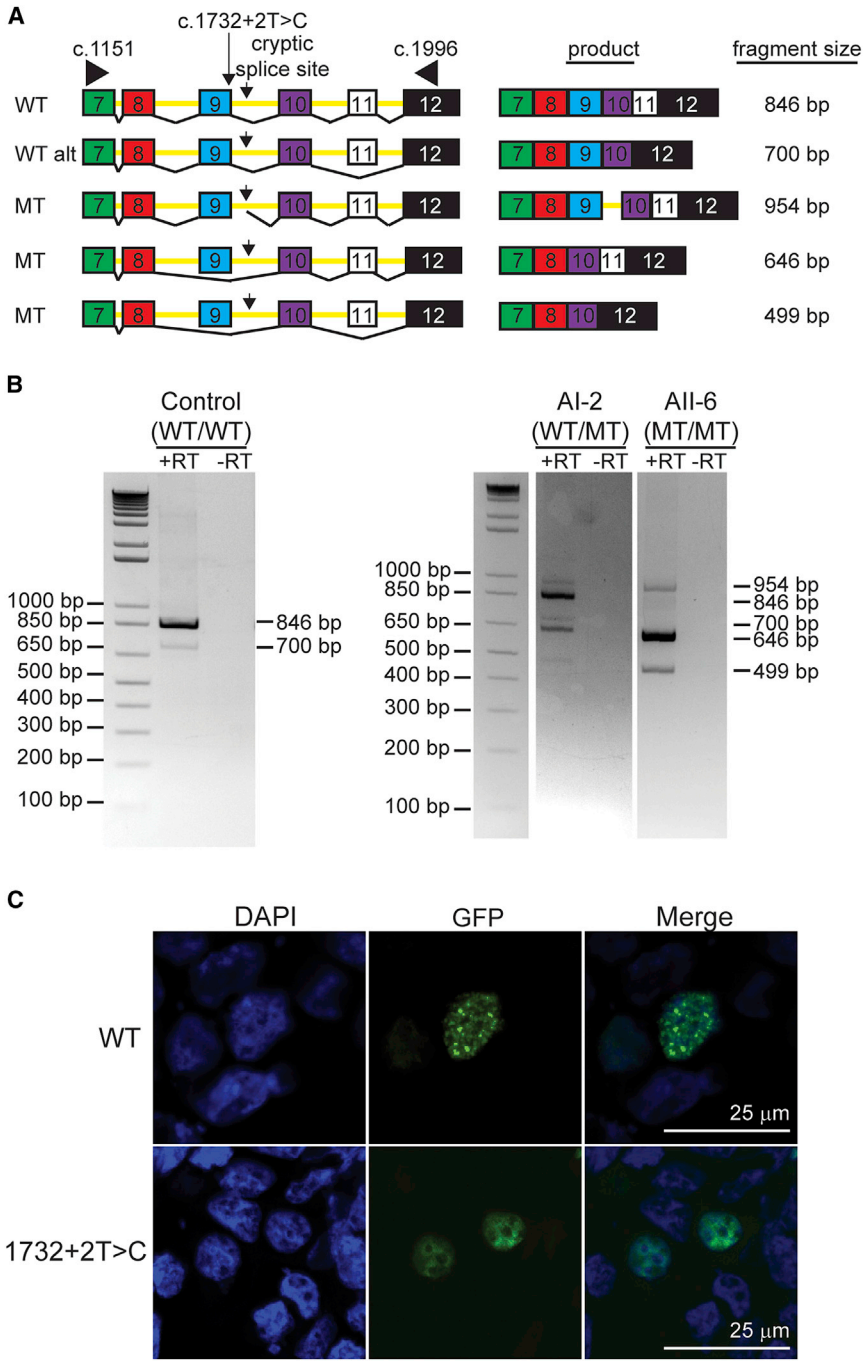

Figure 2. *MCM9* c.1732+2T>C Results in Abnormal Alternative Splicing and Prevents MCM9 Foci Formation at Sites of DNA Damage

(A) Schematic of primer design to detect splicing aberrations and band sizes of each product analyzed. Wild-type products are predicted to produce an 846 bp fragment and a 700 bp fragment resulting from a known alternative splice variant lacking exon 11. The 954 bp fragment is an abnormal splicing product that contains 108 bp of intron 9 and is predicted to introduce a premature stop codon. The 646 bp fragment is an abnormal splicing product that has a deletion of exon 9, and the smaller, 499 bp fragment lacks both exons 9 and 11.

(B) Representative gel image of DNA products fractionated on agarose gel after PCR amplification of cDNA derived from RNA of lymphoblastoid cell lines from an unrelated wild-type control individual, a heterozygous mutation carrier (AI-2), and an affected homozygous mutation carrier (AII-6). Primers used (shown in A) were 5′-GATCTACTAGTGCAGGTCT GACG-3′ (c.1151 forward) and 5′-GCA CACTCTGATTCTGTAACCTTT-3′ (c.1996 reverse). Wild-type control cells and the heterozygous carrier (AI-2) showed both the 846 bp and the 700 bp expected isoforms. The abnormal splicing variants induced by the c.1732T>C mutation were found in the heterozygous mother (AI-2) and the homozygous affected daughter (AII-6). Sanger sequencing verified the abnormal splicing products (Figure S3).

(C) Human embryonic kidney 293T cells were seeded onto 12 cm^2 glass coverslips coated in poly-L-lysine and cultured under standard conditions. Transient transfection of either wild-type MCM9-GFP or altered MCM9-GFP (c.1732+2T>C) into 293T cells was performed with Lipofectamine 2000 (Invitrogen) according to the manufacturer's directions, and DNA damage was induced by cell exposure to 300 nM mitomycin C (MMC) for 6 hr the following day. Coverslips were rinsed twice in PBS, fixed with 3% paraformaldehyde for 15 min, and incubated in PBS with 20% SDS and 10% Triton X-100 for 15 min. Coverslips were mounted with Fluoroshield + DAPI (Sigma) and imaged with an Olympus Fluoview 500 or Olympus Provis AX70 confocal microscope. Nuclei were counterstained with DAPI (blue). Foci formed in 293T cells expressing wild-type MCM9, but not in cells expressing altered MCM9. Representative confocal images taken with a 40× objective are shown. Scale bars represent 25 μm.

lacking the winged helix domain and a unique C-terminal extension might be produced (RefSeq NP_060166.2). The 646 bp fragment was a result of abnormal splicing that skipped exon 9 (Figures S3C and S4C) and is predicted to delete 68 amino acids. Exon 9 encodes a portion of MCM9 that is homologous to the sensor 2 domain of the archaeal MCM ATPase domain (Figure 1D). The sensor 2 domain binds the gamma phosphate of ATP and facilitates ATP binding within the active site.[12,13] The 499 bp fragment resulted from alternative splicing that skipped both exons 9 and 11 (Figures S3B and S3C). Our results show that *MCM9* c.1732+2T>C causes abnormal splicing products predicted to disrupt MCM9 function.

MCM9-containing complexes are known to form foci at sites of DNA damage.[14] To determine whether the

c.1732+2T>C mutation affects the ability of MCM9 to form foci at sites of DNA damage, we generated an MCM9-GFP cDNA construct lacking exon 9 (c.1732+2T>C). We cloned human wild-type *MCM9* into pEGFPC2 (Clontech) in frame with the N-terminal GFP tag by using XhoI and SalI. pEGFPC2-MCM9 c.1732+2T>C was generated by QuikChange (Agilent), which introduced an SphI site for screening. Human embryonic kidney 293T cells were transfected with either wild-type MCM9-GFP or altered MCM9-GFP (c.1732+2T>C), treated with 300 nM mitomycin C (MMC) for 6 hr, and prepared for imaging of GFP signal. GFP foci were counted in 15 cells per experiment. In damaged cells expressing wild-type MCM9-GFP, GFP accumulation was primarily nuclear—an average of 20 ± 3 (SD) nuclear GFP foci per cell formed at sites of DNA damage (Figure 2C, top). In MMC-exposed cells expressing altered MCM9-GFP, GFP signal was localized to the nucleus, but foci could not be found at sites of DNA damage (Figure 2C, bottom). These studies indicate that the *MCM9* c.1732+2T>C pathogenic variant, lacking exon 9, inhibits MCM9 from being recruited to sites of DNA damage.

In family B, we conducted WES on the unaffected daughter (BII-3), both parents (BI-1 and BI-2), and the affected daughter (BII-1) by using the same methodology as described for family A. After variant filtration, there remained 11 variants that fit the homozygous autosomal-recessive model (Table S5). Of these 11, only the *MCM9* variant (c.394C>T [p.Arg132*]) was not present in either the NHLBI Exome Variant Server or 1000 Genomes (Figures 1C and 1D). The variant was confirmed by Sanger Sequencing (Figure 1B, bottom) and was absent in 200 fertile women. This alteration changes a highly conserved residue to a premature stop codon, presumably resulting in loss of functional protein.

During gametogenesis, MCM9 is critical for homologous recombination (HR) in the repair of DNA double-stranded breaks (DSBs) and stabilization of broken or stalled DNA replication forks.[14–19] *Mcm9*-deficient mice have gonadal failure, and fibroblasts from these mice show hypersensitivity to agents that induce DSBs and DNA crosslinks (i.e., ionizing radiation and MMC), resulting in a higher number of broken chromosomes, a hallmark of genomic instability.[19] We assayed DNA-repair capabilities of lymphocytes derived from a single unrelated control individual, unaffected individuals (AII-2, BI-2, and BII-3; Figure 3A), and affected individuals (AII-4, AII-6, and BII-1; Figure 3B and 3C) as previously described.[20] Within-family comparisons suggested a trend where we observed significantly more chromosomal breaks in cells from affected individuals from either family than in cells from the control individual (Figures 3D and 3E). This trend was more apparent as MMC concentrations increased. Treatment with 50 nM MMC induced significant numbers of chromosomal breaks in cells homozygous for the c.394C>T mutation from BII-1, but not in cells from the unrelated control individual ($p = 6.93 \times 10^{-5}$) or heterozygous parent BI-2 ($p = 2.69 \times 10^{-5}$; Figure 3E). Treatment with 150 nM MMC revealed significantly more chromosomal breaks in cells from individuals homozygous for the c.1732+2T>C and c.394C>T mutations (AII-4, AII-6, or BII-1) than in cells from the unrelated control individual ($p = 2.6 \times 10^{-7}$, $p = 1.6 \times 10^{-14}$, and $p = 3.58 \times 10^{-8}$, respectively) or heterozygous carriers (AII-4 versus AII-2, $p = 2.6 \times 10^{-7}$; AII-6 versus AII-2, $p = 5.4 \times 10^{-14}$; BII-1 versus BI-2, $p = 3.24 \times 10^{-8}$; Figures 3D and 3E). Treatment with 300 nM MMC revealed more chromosomal breaks in cells from affected individuals of either family than in cells from the control individual (AII-4 versus control, $p = 7.5 \times 10^{-8}$; AII-6 versus control, $p = 1.6 \times 10^{-7}$; BII-1 versus control, $p = 6.9 \times 10^{-5}$) or heterozygous family members (AII-4 versus AII-2, $p = 7.6 \times 10^{-8}$; AII-6 versus AII-2, $p = 1.5 \times 10^{-7}$; BII-1 versus BI-2, $p = 5.5 \times 10^{-7}$; BII-1 versus BII-3, $p = 1.2 \times 10^{-6}$; Figures 3D and 3E). When we compared cells of the affected daughters across both families, BII-1 (c.394C>T) appeared to be more sensitive to chromosomal breakage at 50 nM (average breaks per cell = 1.6 ± 0.9) than AII-4 (c.1732+2T>C; average breaks per cell = 0.6 ± 0.5; $p = 0.001$) or AII-6 (c.1732+2T>C; average breaks per cell = 0.8 ± 0.5; $p = 0.00039$). AII-4 and AII-6 had significantly more breaks then BII-1 at 150 nM (10.5 ± 2.1 [AII-4], 8.1 ± 2.3 [AII-6], and 4.0 ± 1.1 [BII-1]; AII-4 versus BII-1, $p = 7.5 \times 10^{-6}$; AII-6 versus BII-1, $p = 4.96 \times 10^{-8}$). At the highest concentration of MMC, BII-1 (average breaks per cell = 23.5 ± 6.6) had significantly more breaks per cell on average than AII-6 (average breaks per cell = 14.79 ± 9.23; $p = 0.0051$), but not AII-4 (average breaks per cell = 24.1 ± 4.0; $p = 0.81$). Overall, c.394C>T appeared to have a statistically greater effect than c.1732+2T>C on DNA-damage repair in cells treated with 50 nM MMC. At higher MMC concentrations, repair appeared to be equally impaired in cells from homozygous carriers of either *MCM9* mutation. In summary, homozygous carriers of the *MCM9* variants (c.394C>T and c.1732+2T>C) failed to repair DNA damage as effectively as heterozygous carriers or wild-type individuals. Analysis of WES data from affected sisters in either family did not reveal pathogenic variants in genes known to be associated with chromosomal instability and/or ovarian failure (Table S7).

The contribution of single Mendelian genes to idiopathic POF is low, as shown by studies on *SF1* (MIM 601516) and *FOXL2* mutations.[21–24] To determine whether *MCM9* variants underlie idiopathic POF, we investigated the prevalence of *MCM9* mutations in a cohort of 109 idiopathic-POF-affected women (98 European, 6 Hispanic, 3 Indian, 1 African American, 1 of mixed descent) who were recruited at Magee-Womens Hospital. Informed written consent and samples were obtained at the time of recruitment. The study was approved by the institutional review board of the University of Pittsburgh. We amplified *MCM9* exons with the KAPA HiFi HotStart PCR

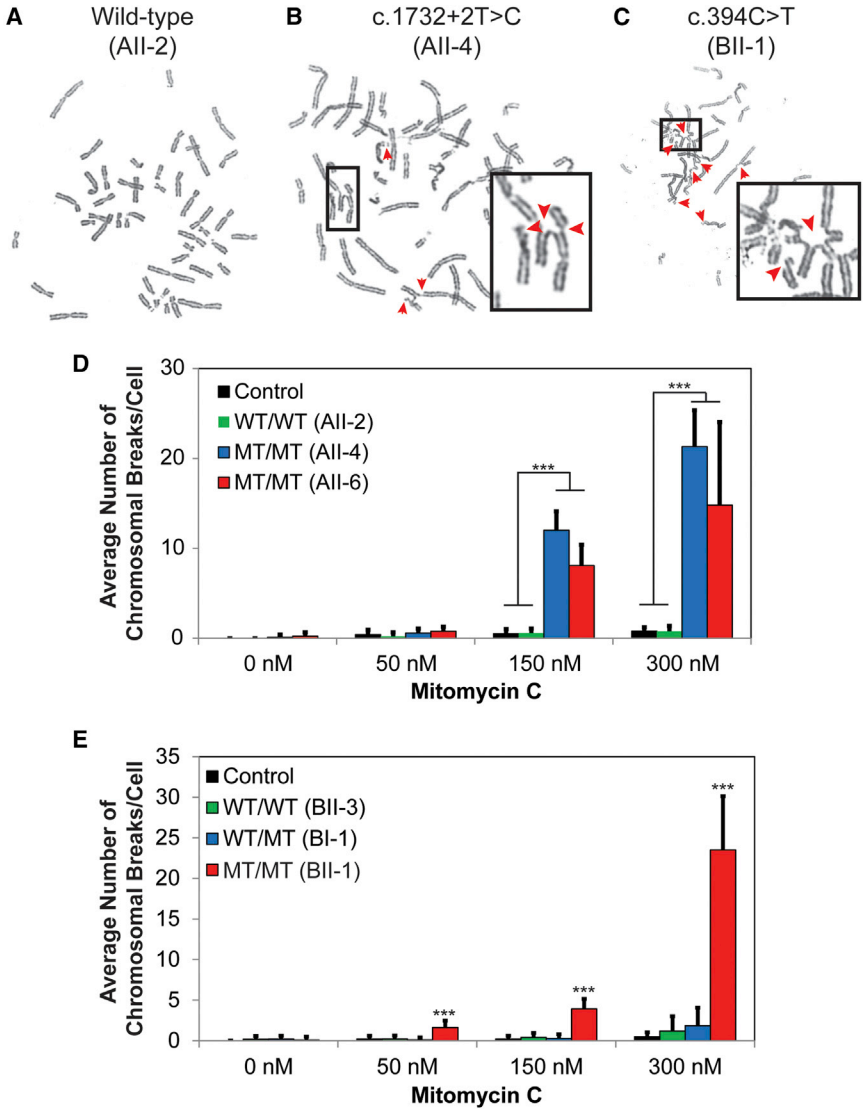

Figure 3. Mutations in Human *MCM9* Impair the Repair of MMC-Induced Chromosomal Breaks

Homozygous *MCM9* mutations c.1732+2T>C and c.394C>T associate with an increased rate of chromosomal breakage. Peripheral lymphocytes were stimulated with phytohaemagglutinin and cultured in the presence of MMC. In brief, cells were cultured in the presence of MMC at a concentration of 0, 50, 150, or 300 nM. Cells were harvested after 72 hr of incubation at 37°C. At least ten metaphase spreads per sample were evaluated for chromosome aberrations and breaks (Table S6).

(A–C) Representative figures of metaphase spreads from (A) wild-type cells, (B) cells with homozygous c.1732+2T>C, and (C) cells with homozygous c.394C>T are shown after treatment with 300 nM MMC. Compared to wild-type cells, homozygous mutant cells showed extensive chromosome damage with numerous breaks, nonhomologous exchanges, chromatid deletions, complex aberrations, and acentric fragments (arrows).

(D and E) The mean numbers of chromosomal breaks per cell were quantified for cells from (D) family A (with the c.1732+2T>C mutation) and (E) family B (with the c.394C>T mutation). Bar graphs show the mean observed number of breaks per cell (±SD) for each MMC concentration. At least ten metaphase cells were studied for affected family members (AII-4, AII-6, and BII-1), unaffected family members (AII-2, BII-3, and BI-2), and a healthy fertile unrelated control female. Single-factor ANOVA was utilized for determining the effect of drug concentration on each cell line. Two-tailed t tests assuming unequal variance were used for comparing two cell lines at a single drug concentration. ***$p < 0.001$. Abbreviations are as follows: MT, mutant; and WT, wild-type.

Kit (Kapa Biosystems) according to the manufacturer's instructions (primers are provided in Table S8). PCR products were sequenced and analyzed with Sequencher (Gene Codes Corporation). Among 109 individuals, we identified eight *MCM9* variants (Tables S9 and S10). All of the variants except one, c.1533C>A (p.Tyr511*), were previously reported as SNPs. All reported SNPs are benign except for one, rs200078427 (c.686T>G [p.Val229Gly]), which is predicted to be probably damaging. We suspect that these SNPs do not account for the POF phenotype because of heterozygosity. Our data suggest that the prevalence of biallelic pathogenic *MCM9* variants is low in women with idiopathic POF.

We combined homozygosity mapping and WES in two unrelated consanguineous families to identify recessive pathogenic variants in *MCM9*. Individuals homozygous for the *MCM9* c.1732+2T>C and c.394C>T pathogenic variants shared a Turner-like phenotype characterized by ovarian insufficiency, short stature, low weight, and genomic instability in somatic cells exposed to MMC. We also showed that cells containing the c.1732+2T>C and c.394C>T variants were impaired in their ability to repair DNA damage, most likely as a result of the inability of MCM9 to be recruited to sites of DNA damage. Minichromosome maintenance proteins MCM2–MCM7 have been implicated in DNA-replication elongation and prereplication-complex formation.[25] MCM8 and MCM9 are two of the last discovered members of the minichromosome maintenance protein homologs and, by association with other MCMs, were initially implicated in DNA replication.[15] Unexpectedly, *Mcm8*- and *Mcm9*-deficient mice show a phenotype (infertility and small gonads) primarily restricted to the germline.[19] In addition, somatic cells exhibit growth defects and chromosomal instability.[19] The phenotype of the three affected individuals from two independent families is very similar to what has been described in mouse knockouts. MCM8 and MCM9 are regulators of germ cell survival, are rapidly induced and

recruited to sites of DNA damage, coregulate each other's stability, and promote RAD51 recruitment to the chromatin.[18,19] The mechanisms of their action, induction, and regulation in homologous recombination remain poorly understood.

In the germline, the MCM8-MCM9 complex is most likely required for the resolution of DSBs that occur during HR between homologous chromosomes in pachytene of meiosis I. Failure to resolve breaks will lead to oocyte death and thus very small or absent ovaries in women homozygous for these mutations. A number of mouse mutants lacking genes involved in meiosis and DNA repair, such as *Dmc1*, *Msh5*, *Stag3*, and *Syce1*, lose oocytes rapidly in part because of their inability to process DSBs.[26–29] Indeed, mutations in *DMC1*, *MSH5*, *STAG3*, and *SYCE1* have been identified in women with POF[28,30,31] and underscore the genetic heterogeneity of POF. DSB genes, including a SNP in *MCM8* (rs16991615), have been implicated in the onset of menopause by genome-wide association studies (GWASs).[32–37] However, no association has been identified between menopause and *MCM9*, including in GWASs.[32] The close physical interdependence of MCM8 and MCM9 shows the importance of this pathway in a spectrum of ovarian functions from gonadal development to menopause.

Genomic-instability syndromes, such as Fanconi anemia,[6] can associate with short stature, hypogonadism, and multiple endocrine dysfunctions.[38] The mechanism of how genomic instability contributes to endocrinopathies has not been elucidated and is most likely linked to complex regulatory networks in the hypothalamic-pituitary-endocrine axes of the body.[38] Heterozygous sisters and mothers have had unremarkable medical histories to date, but future follow-up examinations and phenotyping of additional individuals with *MCM9* variants will be of great importance for understanding their predisposition to other disorders, including endocrine dysfunction and cancer.

Supplemental Data

Supplemental Data include four figures and ten tables and can be found with this article online at http://dx.doi.org/10.1016/j.ajhg.2014.11.002.

Acknowledgments

We thank the affected individuals and their families for their participation in this research study on the genetics of premature ovarian failure. We thank the Cytogenetics Laboratory at Magee-Womens Hospital for their assistance with the chromosomal-breakage studies, the Cell Culture and Cytogenetics Facility at the University of Pittsburgh Cancer Institute for producing the Epstein-Barr virus cell line, and the Clinical Genomics Laboratory for whole-exome sequencing. Funding was provided by the National Institute of Child Health and Human Development (R01HD070647 and R21HD074278 to A.R.), the Magee-Womens Research Institute Postdoctoral Fellowship (M.A.W.-T.), and Cukurova University Scientific Research Projects.

Received: August 25, 2014
Accepted: November 6, 2014
Published: December 4, 2014

Web Resources

The URLs for data presented herein are as follows:

1000 Genomes, http://www.1000genomes.org
dbSNP, http://www.ncbi.nlm.nih.gov/SNP/
Gene Expression Omnibus, http://www.ncbi.nlm.nih.gov/geo
Homozygosity Mapper, http://www.homozygositymapper.org
NHLBI Exome Sequencing Project (ESP) Exome Variant Server, http://evs.gs.washington.edu/EVS/
Online Mendelian Inheritance in Man (OMIM), http://www.omim.org/
PolyPhen-2, http://genetics.bwh.harvard.edu/pph2/
RefSeq, http://www.ncbi.nlm.nih.gov/refseq/
Sequencing Read Archive, http://www.ncbi.nlm.nih.gov/sra
SIFT, http://sift.jcvi.org/
UCSC Genome Browser, http://genome.ucsc.edu/

Accession Numbers

All whole-exome sequencing data have been deposited in the Sequence Reads Archive under accession number SRP047423. Data from the combination SNP and CGH array has been deposited in the Gene Expression Omnibus under accession number GSE62347. *MCM9* variants identified in this paper have been deposited in dbSNP under accession numbers rs587777871 (c.1732+2T>C), rs587777872 (c.394C>T), and rs587777873 (c.1533C>A).

References

1. Nelson, L.M. (2009). Clinical practice. Primary ovarian insufficiency. N. Engl. J. Med. *360*, 606–614.
2. Rafique, S., Sterling, E.W., and Nelson, L.M. (2012). A new approach to primary ovarian insufficiency. Obstet. Gynecol. Clin. North Am. *39*, 567–586.
3. Vegetti, W., Grazia Tibiletti, M., Testa, G., Alagna, F., Castoldi, E., Taborelli, M., Motta, T., Bolis, P.F., Dalprà, L., and Crosignani, P.G.; de Lauretis Yankowski (1998). Inheritance in idiopathic premature ovarian failure: analysis of 71 cases. Hum. Reprod. *13*, 1796–1800.
4. Practice Committee of American Society for Reproductive Medicine (2008). Current evaluation of amenorrhea. Fertil. Steril. *90* (*Suppl*), S219–S225.
5. German, J. (1993). Bloom syndrome: a mendelian prototype of somatic mutational disease. Medicine (Baltimore) *72*, 393–406.
6. Wong, J.C., Alon, N., Mckerlie, C., Huang, J.R., Meyn, M.S., and Buchwald, M. (2003). Targeted disruption of exons 1 to 6 of the Fanconi Anemia group A gene leads to growth retardation, strain-specific microphthalmia, meiotic defects and primordial germ cell hypoplasia. Hum. Mol. Genet. *12*, 2063–2076.
7. Barlow, C., Hirotsune, S., Paylor, R., Liyanage, M., Eckhaus, M., Collins, F., Shiloh, Y., Crawley, J.N., Ried, T., Tagle, D., and

Wynshaw-Boris, A. (1996). Atm-deficient mice: a paradigm of ataxia telangiectasia. Cell *86*, 159–171.
8. Maraschio, P., Peretti, D., Lambiase, S., Lo Curto, F., Caufin, D., Gargantini, L., Minoli, L., and Zuffardi, O. (1986). A new chromosome instability disorder. Clin. Genet. *30*, 353–365.
9. Li, H., and Durbin, R. (2010). Fast and accurate long-read alignment with Burrows-Wheeler transform. Bioinformatics *26*, 589–595.
10. Li, H., and Durbin, R. (2009). Fast and accurate short read alignment with Burrows-Wheeler transform. Bioinformatics *25*, 1754–1760.
11. Jeffries, E.P., Denq, W.H., Bartko, J.C., and Trakselis, M.A. (2013). Identification, quantification, and evolutionary analysis of a novel isoform of MCM9. Gene *519*, 41–49.
12. Bochman, M.L., and Schwacha, A. (2009). The Mcm complex: unwinding the mechanism of a replicative helicase. Microbiol. Mol. Biol. Rev. *73*, 652–683.
13. Brewster, A.S., Wang, G., Yu, X., Greenleaf, W.B., Carazo, J.M., Tjajadi, M., Klein, M.G., and Chen, X.S. (2008). Crystal structure of a near-full-length archaeal MCM: functional insights for an AAA+ hexameric helicase. Proc. Natl. Acad. Sci. USA *105*, 20191–20196.
14. Nishimura, K., Ishiai, M., Horikawa, K., Fukagawa, T., Takata, M., Takisawa, H., and Kanemaki, M.T. (2012). Mcm8 and Mcm9 form a complex that functions in homologous recombination repair induced by DNA interstrand crosslinks. Mol. Cell *47*, 511–522.
15. Gozuacik, D., Chami, M., Lagorce, D., Faivre, J., Murakami, Y., Poch, O., Biermann, E., Knippers, R., Bréchot, C., and Paterlini-Bréchot, P. (2003). Identification and functional characterization of a new member of the human Mcm protein family: hMcm8. Nucleic Acids Res. *31*, 570–579.
16. Volkening, M., and Hoffmann, I. (2005). Involvement of human MCM8 in prereplication complex assembly by recruiting hcdc6 to chromatin. Mol. Cell. Biol. *25*, 1560–1568.
17. Kinoshita, Y., Johnson, E.M., Gordon, R.E., Negri-Bell, H., Evans, M.T., Coolbaugh, J., Rosario-Peralta, Y., Samet, J., Slusser, E., Birkenbach, M.P., and Daniel, D.C. (2008). Colocalization of MCM8 and MCM7 with proteins involved in distinct aspects of DNA replication. Microsc. Res. Tech. *71*, 288–297.
18. Park, J., Long, D.T., Lee, K.Y., Abbas, T., Shibata, E., Negishi, M., Luo, Y., Schimenti, J.C., Gambus, A., Walter, J.C., and Dutta, A. (2013). The MCM8-MCM9 complex promotes RAD51 recruitment at DNA damage sites to facilitate homologous recombination. Mol. Cell. Biol. *33*, 1632–1644.
19. Lutzmann, M., Grey, C., Traver, S., Ganier, O., Maya-Mendoza, A., Ranisavljevic, N., Bernex, F., Nishiyama, A., Montel, N., Gavois, E., et al. (2012). MCM8- and MCM9-deficient mice reveal gametogenesis defects and genome instability due to impaired homologous recombination. Mol. Cell *47*, 523–534.
20. Oostra, A.B., Nieuwint, A.W., Joenje, H., and de Winter, J.P. (2012). Diagnosis of fanconi anemia: chromosomal breakage analysis. Anemia *2012*, 238731.
21. Harris, S.E., Chand, A.L., Winship, I.M., Gersak, K., Aittomäki, K., and Shelling, A.N. (2002). Identification of novel mutations in FOXL2 associated with premature ovarian failure. Mol. Hum. Reprod. *8*, 729–733.
22. Kuo, F.T., Bentsi-Barnes, I.K., Barlow, G.M., and Pisarska, M.D. (2011). Mutant Forkhead L2 (FOXL2) proteins associated with premature ovarian failure (POF) dimerize with wild-type FOXL2, leading to altered regulation of genes associated with granulosa cell differentiation. Endocrinology *152*, 3917–3929.
23. Ni, F., Wen, Q., Wang, B., Zhou, S., Wang, J., Mu, Y., Ma, X., and Cao, Y. (2010). Mutation analysis of FOXL2 gene in Chinese patients with premature ovarian failure. Gynecol. Endocrinol. *26*, 246–249.
24. Lakhal, B., Ben-Hadj-Khalifa, S., Bouali, N., Braham, R., Hatem, E., and Saad, A. (2012). Mutational screening of SF1 and WNT4 in Tunisian women with premature ovarian failure. Gene *509*, 298–301.
25. Vijayraghavan, S., and Schwacha, A. (2012). The eukaryotic Mcm2-7 replicative helicase. Subcell. Biochem. *62*, 113–134.
26. Yoshida, K., Kondoh, G., Matsuda, Y., Habu, T., Nishimune, Y., and Morita, T. (1998). The mouse RecA-like gene Dmc1 is required for homologous chromosome synapsis during meiosis. Mol. Cell *1*, 707–718.
27. de Vries, S.S., Baart, E.B., Dekker, M., Siezen, A., de Rooij, D.G., de Boer, P., and te Riele, H. (1999). Mouse MutS-like protein Msh5 is required for proper chromosome synapsis in male and female meiosis. Genes Dev. *13*, 523–531.
28. Caburet, S., Arboleda, V.A., Llano, E., Overbeek, P.A., Barbero, J.L., Oka, K., Harrison, W., Vaiman, D., Ben-Neriah, Z., García-Tuñón, I., et al. (2014). Mutant cohesin in premature ovarian failure. N. Engl. J. Med. *370*, 943–949.
29. Bolcun-Filas, E., Hall, E., Speed, R., Taggart, M., Grey, C., de Massy, B., Benavente, R., and Cooke, H.J. (2009). Mutation of the mouse Syce1 gene disrupts synapsis and suggests a link between synaptonemal complex structural components and DNA repair. PLoS Genet. *5*, e1000393.
30. Mandon-Pépin, B., Touraine, P., Kuttenn, F., Derbois, C., Rouxel, A., Matsuda, F., Nicolas, A., Cotinot, C., and Fellous, M. (2008). Genetic investigation of four meiotic genes in women with premature ovarian failure. Eur. J. Endocrinol. *158*, 107–115.
31. de Vries, L., Behar, D.M., Smirin-Yosef, P., Lagovsky, I., Tzur, S., and Basel-Vanagaite, L. (2014). Exome Sequencing Reveals SYCE1 Mutation Associated With Autosomal Recessive Primary Ovarian Insufficiency. J. Clin. Endocrinol. Metab. *99*, E2129–E2132.
32. Stolk, L., Perry, J.R., Chasman, D.I., He, C., Mangino, M., Sulem, P., Barbalic, M., Broer, L., Byrne, E.M., Ernst, F., et al. (2012). Meta-analyses identify 13 loci associated with age at menopause and highlight DNA repair and immune pathways. Nat. Genet. *44*, 260–268.
33. Schuh-Huerta, S.M., Johnson, N.A., Rosen, M.P., Sternfeld, B., Cedars, M.I., and Reijo Pera, R.A. (2012). Genetic markers of ovarian follicle number and menopause in women of multiple ethnicities. Hum. Genet. *131*, 1709–1724.
34. Chen, C.T., Fernández-Rhodes, L., Brzyski, R.G., Carlson, C.S., Chen, Z., Heiss, G., North, K.E., Woods, N.F., Rajkovic, A., Kooperberg, C., and Franceschini, N. (2012). Replication of loci influencing ages at menarche and menopause in Hispanic women: the Women's Health Initiative SHARe Study. Hum. Mol. Genet. *21*, 1419–1432.
35. He, C., Kraft, P., Chasman, D.I., Buring, J.E., Chen, C., Hankinson, S.E., Paré, G., Chanock, S., Ridker, P.M., and Hunter, D.J. (2010). A large-scale candidate gene association study of age at menarche and age at natural menopause. Hum. Genet. *128*, 515–527.
36. Carty, C.L., Spencer, K.L., Setiawan, V.W., Fernandez-Rhodes, L., Malinowski, J., Buyske, S., Young, A., Jorgensen, N.W., Cheng, I., Carlson, C.S., et al. (2013). Replication of genetic

loci for ages at menarche and menopause in the multi-ethnic Population Architecture using Genomics and Epidemiology (PAGE) study. Hum. Reprod. *28*, 1695–1706.

37. Spencer, K.L., Malinowski, J., Carty, C.L., Franceschini, N., Fernández-Rhodes, L., Young, A., Cheng, I., Ritchie, M.D., Haiman, C.A., Wilkens, L., et al. (2013). Genetic variation and reproductive timing: African American women from the Population Architecture using Genomics and Epidemiology (PAGE) Study. PLoS ONE *8*, e55258.
38. Giri, N., Batista, D.L., Alter, B.P., and Stratakis, C.A. (2007). Endocrine abnormalities in patients with Fanconi anemia. J. Clin. Endocrinol. Metab. *92*, 2624–2631.